

AD_____

Award Number: W81XWH-04-1-0340

TITLE: Near Infrared Spectroscopy for Improving Breast Core Needle Biopsy

PRINCIPAL INVESTIGATOR: Torre Michelle Bydlon

CONTRACTING ORGANIZATION: Duke University
Durham, NC 27708

REPORT DATE: September 2008

TYPE OF REPORT: Annual Summary

PREPARED FOR: U.S. Army Medical Research and Materiel Command
Fort Detrick, Maryland 21702-5012

DISTRIBUTION STATEMENT: Approved for Public Release;
Distribution Unlimited

The views, opinions and/or findings contained in this report are those of the author(s) and should not be construed as an official Department of the Army position, policy or decision unless so designated by other documentation.

REPORT DOCUMENTATION PAGE				Form Approved OMB No. 0704-0188	
Public reporting burden for this collection of information is estimated to average 1 hour per response, including the time for reviewing instructions, searching existing data sources, gathering and maintaining the data needed, and completing and reviewing this collection of information. Send comments regarding this burden estimate or any other aspect of this collection of information, including suggestions for reducing this burden to Department of Defense, Washington Headquarters Services, Directorate for Information Operations and Reports (0704-0188), 1215 Jefferson Davis Highway, Suite 1204, Arlington, VA 22202-4302. Respondents should be aware that notwithstanding any other provision of law, no person shall be subject to any penalty for failing to comply with a collection of information if it does not display a currently valid OMB control number. PLEASE DO NOT RETURN YOUR FORM TO THE ABOVE ADDRESS.					
1. REPORT DATE (DD-MM-YYYY) 01-09-2008		2. REPORT TYPE Annual Summary		3. DATES COVERED (From - To) 1 SEP 2007 - 31 AUG 2008	
4. TITLE AND SUBTITLE Near Infrared Spectroscopy for Improving Breast Core Needle Biopsy				5a. CONTRACT NUMBER	
				5b. GRANT NUMBER W81XWH-04-1-0340	
				5c. PROGRAM ELEMENT NUMBER	
6. AUTHOR(S) Torre Michelle Bydlon E-Mail: tmb14@duke.edu				5d. PROJECT NUMBER	
				5e. TASK NUMBER	
				5f. WORK UNIT NUMBER	
7. PERFORMING ORGANIZATION NAME(S) AND ADDRESS(ES) Duke University Durham, NC 27708				8. PERFORMING ORGANIZATION REPORT NUMBER	
9. SPONSORING / MONITORING AGENCY NAME(S) AND ADDRESS(ES) U.S. Army Medical Research and Materiel Command Fort Detrick, Maryland 21702-5012				10. SPONSOR/MONITOR'S ACRONYM(S)	
				11. SPONSOR/MONITOR'S REPORT NUMBER(S)	
12. DISTRIBUTION / AVAILABILITY STATEMENT Approved for Public Release; Distribution Unlimited					
13. SUPPLEMENTARY NOTES					
14. ABSTRACT The objective of the proposed research is to develop a device to reduce the frequency of breast re-excision surgery in patients with breast malignancies. The purpose of Task 2 was to build and test a fiber optic probe with two imaging channels. The fiber geometry of this probe showed that collected data was repeatable and accurate at extracting known optical properties. The purpose of Task 3 was to build a multi-channel imaging probe which was constructed with 19, 200um illumination fibers and 4, 200um collection fibers. The objective of Task 4 was to test the multi-channel imaging probe on tissue phantom data and partial mastectomy specimens. Tissue phantom studies revealed that data can be accurately extracted with the current imaging system and multi-channel fiber optic probe. To date, partial mastectomy margins have been imaged on 43 patients and show statistically significant differences between negative and close/positive surgical margins.					
15. SUBJECT TERMS Margin, cross-talk, spectral imaging system, diffuse reflectance, Monte Carlo, signal-to-noise ratio					
16. SECURITY CLASSIFICATION OF:			17. LIMITATION OF ABSTRACT	18. NUMBER OF PAGES	19a. NAME OF RESPONSIBLE PERSON
a. REPORT	b. ABSTRACT	c. THIS PAGE			USAMRMC
U	U	U	UU	22	19b. TELEPHONE NUMBER (include area code)

Table of Contents

Introduction.....	1
Body.....	2
Key Research Accomplishments.....	15
Reportable Outcomes.....	15
Conclusions.....	15
References.....	16
Appendix.....	17

Introduction

In 2008, an estimated 182,460 women in the United States will be diagnosed with invasive breast cancer.¹ Breast cancer is the second leading cause of cancer-related deaths in women in the U.S..² Though regional differences exist, 45-60% of women with early stage invasive breast cancer and/or CIS receive breast conserving surgery (BCS) each year.³ BCS involves removal of malignant tissue with a surrounding margin of normal breast tissue. After pathologic assessment, the results are reviewed and a decision made for a re-excision partial mastectomy versus simple mastectomy if there is evidence of positive or close margins. A positive or close margin is where there are non-invasive or invasive tumor cells within 2.0 mm of the edge of the tissue excised. Currently the rate of re-excision post-BCS can be as high as 70%.⁴ Thus, there is an unmet clinical need for effective intraoperative assessment of tumor margins in patients with breast cancer.

The objective of the proposed research is to develop a device to reduce the frequency of breast re-excision surgery and the risk of local recurrence in patients with invasive and non-invasive breast malignancy. The purpose of Tasks 1-3 is to develop a multi-channel optical device for intraoperative imaging of each margin in specimens freshly excised from patients undergoing breast conserving surgery. The device will be used to collect diffuse reflectance spectrum in the visible wavelength range from each of multiple pixels. The spectra will be analyzed by an inverse Monte Carlo model developed by our group to extract optical absorption and scattering properties from the spectral data at each pixel which can then be translated into maps of tissue biochemical and structural properties.^{5,6} The endogenous absorbers in tissue that can be extracted include oxygenated and deoxygenated hemoglobin, beta carotene, electron carriers and structural proteins. The device can also be used to image exogenous sources of absorption (organic dyes such as lymphazurin) and scattering (nanoparticles) and thus can provide the concentration and distribution of these agents in tissue. These features will be used to identify positive margins. This information will guide the surgeon to complete the surgery, if margins are negative, or re-excite additional tissue from areas in the cavity corresponding to the specific margins that are positive, thus preventing repeat surgery and the risk of local recurrence. The purpose of Tasks 4 and 5 is to measure surgical margins with the developed multi-channel probe, identify specific parameters that are statistically different between negative and close/positive margins, and create a model to predict surgical margin status.

The results from Tasks 1 and 2 were reported previously. The remainder of the work from Task 2 along with the results from Task 3 and 4 are presented below.

Body

In the past year the project has deviated slightly from the proposed Statement of Work. Task 2 was completed except for part C. The amount of hemoglobin required to make a tissue phantom with at least a 10mm separation distance between channels would be rather costly. Therefore, simulations from the previous report were relied upon to determine the separation distance between individual channels to minimize tissue crosstalk. Task 3 and 4 have also been completed, however, rather than constructing a 25 channel imaging probe an 8 channel imaging probe was made. The same amount of tissue area can be covered with the 8 channel imaging probe as the 25 channel if the probe is moved around. This slightly increases the amount of time it takes to survey a single margin, however, it is more cost effective for a device that is being used to test how well an imaging probe can diagnose surgical margin status. If the 8 channel imaging probe shows reliable results then a larger imaging probe can be constructed in the future.

The objective of Task 2 was to build a two-channel imaging probe to test the conceptual design without having to build the entire multi-channel probe. As reported previously, the 2-channel probe, seen below in Figure 1, was constructed by our group.

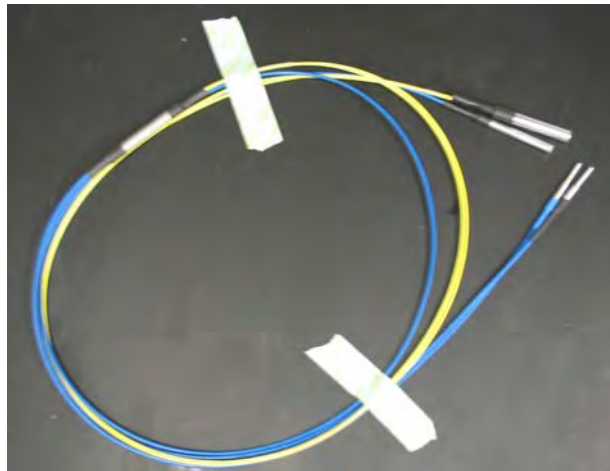


Figure 1. Photo of the completed two-channel fiber optic probe.

The repeatability of the 2 channel probe was tested by taking 10 serial measurements in a tissue phantom with each channel. This can be seen in Figure 2 a,b below. From the images both channels show that almost all 10 measurements overlap. The mean (Figure 2c) and the standard deviation (Figure 2d) were calculated for the 10 measurements. Signal to noise ratio (SNR) was also calculated, Figure 3, as being greater than 100 for both channels, meaning that there is little deviation from the mean and both channels are repeatable.

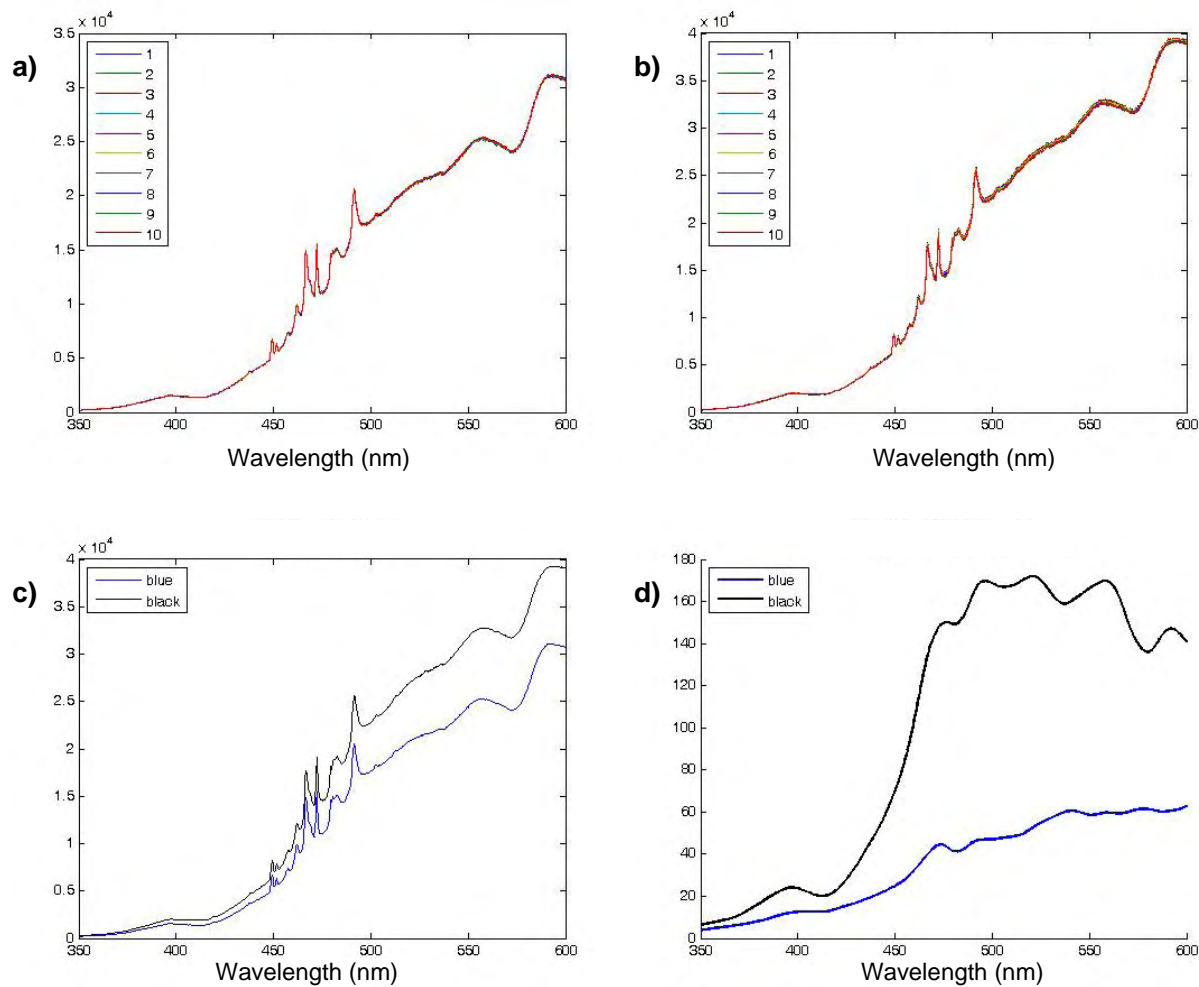


Figure 2. a) Repeatability of channel 1 with 10 serial measurements, b) repeatability of channel 2 with 10 serial measurements, c) mean of both channels, d) standard deviation of both channels

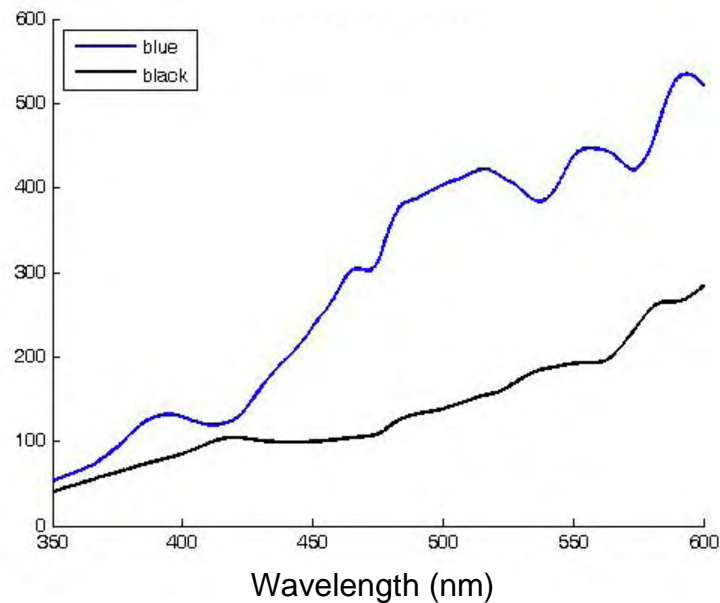


Figure 3. Signal to noise ratio of repeatability studies versus wavelength

Tissue phantoms consisting of hemoglobin and polystyrene spheres were made with an absorption coefficient range of 0.93 – 2.13 cm⁻¹ and a reduced scattering range of 12.43 – 13.3 cm⁻¹. The average percent error between the extracted optical properties and the known values across all phantoms for the absorption coefficient was 22% and for the reduced scattering coefficient was 1%. Although the percent error for the absorption coefficient was slightly high it was only off in one phantom. Therefore, one titration of hemoglobin may have been miscalculated. If this one phantom was removed the average percent error decreased to 4.5%. These results showed that the 2 channel probe was accurate at extracting optical properties.

The goal of Task 3 was to build a multi-channel imaging probe. An 8 channel fiber optic probe was built by Romack Inc.. A photo of the 8 channel probe can be seen in Figure 4. Each channel of the probe has 19, 200um illumination fibers and 4, 200um collection fibers. As determined from the work reported last year, each channel must be separated by 10mm to avoid crosstalk between channels. An adaptor was made by a machine shop here at Duke University to secure each channel of the probe 10mm apart in 4x2 array, as seen in Figure 5.



Figure 4. Photo of the completed 8 channel fiber optic probe in its adaptor.

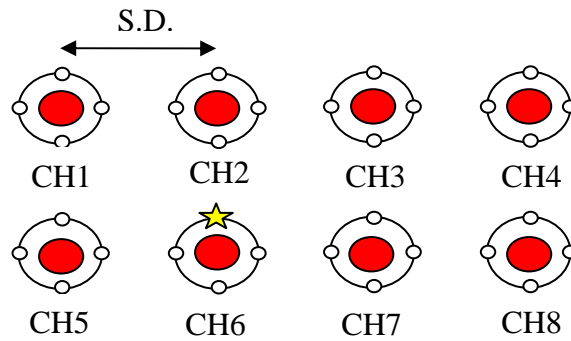


Figure 5. Arrangement of the channels on the tissue with a 10mm separation distance (S.D.), each white circle depicts a collection fiber and the red circle at the center consists of 19, 200 μ m illumination fibers.

The fiber optic probe is coupled to a Xenon lamp and monochromator on one end and spectrometer and 1024x256 pixel CCD on the other end. A block diagram of this system can be seen in Figure 6.

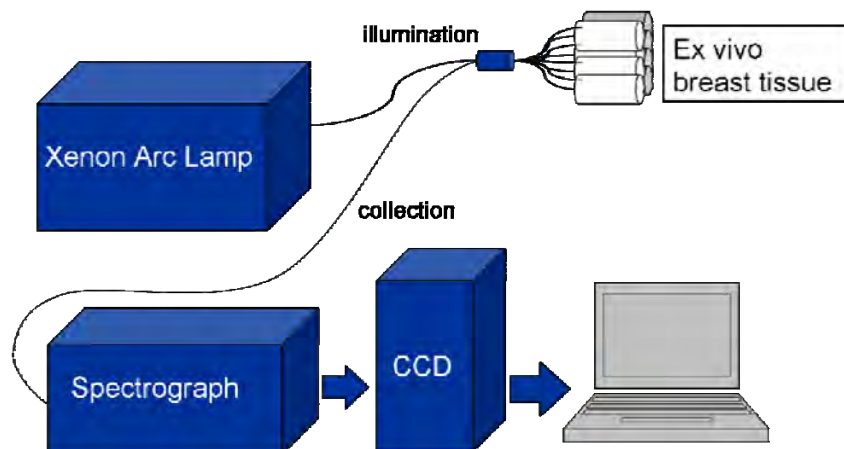


Figure 6. Block diagram of the imaging probe and instrumentation.

The goal of Task 4 was to test the fiber optic probe and system on partial mastectomy specimens. A tissue phantom study was conducted to show accurate extractions of a range of absorption and reduced scattering coefficients found in the breast. Liquid phantoms consisted of hemoglobin and polystyrene spheres. Twelve phantoms were made with an absorption coefficient range of 0.16-2.0 cm^{-1} and a reduced scattering coefficient range of 13.3-20.77 cm^{-1} .⁷ Phantom data was analyzed by running an inverse Monte Carlo model, created by our group, to extract the optical properties of the phantoms.^{5,6} Percent errors were computed between the extracted values and the actual optical properties; these percent errors for the absorption and reduced scattering properties for each channel are shown in Table 1. The comparable errors across each channel indicate that there is minimal crosstalk between channels in the configuration in which it is used to image breast tumor margins and that optical properties can be accurately extracted.

	Channel #									
	1	2	3	4	5	6	7	8	Average	Variance
μ_a	11.41	11.62	10.89	12.56	13.58	18.51	12.84	14.99	13.30	6.15
μ_s'	3.65	2.93	3.07	3.93	3.13	3.30	3.30	3.37	3.34	0.10

Table 1. Average percent errors across all phantoms for each channel. Optical property ranges – μ_a (0.16-2 cm^{-1}), μ_s' (13.3-20.77 cm^{-1}).

An ex-vivo clinical study to image breast tumor margins has been done on 43 patients undergoing breast conserving surgery. 35 of these patients were used in the data analysis. 2 patients were removed due to instrumentation errors. Patients were also removed if the optically imaged margin was pathologically negative but the patient had a pathologically positive margin elsewhere; this accounted for 6 patients.

Partial mastectomy (lumpectomy) specimens were excised and oriented by the surgeon using clips or sutures placed at the center of multiple margins. The specimen was then placed in a plexi-glass box (10-15 minutes post-excision) with the clip or suture at the center of the box face to maintain surgical orientation for each margin of the specimen. Diffuse reflectance measurements (400-600nm) were collected from sites 5 mm apart until the whole margin had been scanned, taking 8 measurements simultaneously. If time permitted, a second or third margin was imaged. The margin measured was chosen by either what the surgeon believed was most likely to be positive or in the order of posterior, anterior, superior, medial, inferior, then lateral. Table 2 shows the percentage of positive margins stratified by the margin for our study. This agrees with what is found in the literature that anterior and posterior are most likely positive. The four corners of the measured margin were inked for pathology to outline the imaged area, as shown in Figure 7. Table 3 shows the percentage of margins that were correctly oriented by our group for pathology. For the most part, our group is able to orient each specimen correctly.

Margin	% of Positive Margins
Anterior	22%
Inferior	10%
Lateral	4%
Medial	16%
Posterior	30%
Superior	18%

Table 2. The percentage of margins that are path-positive.

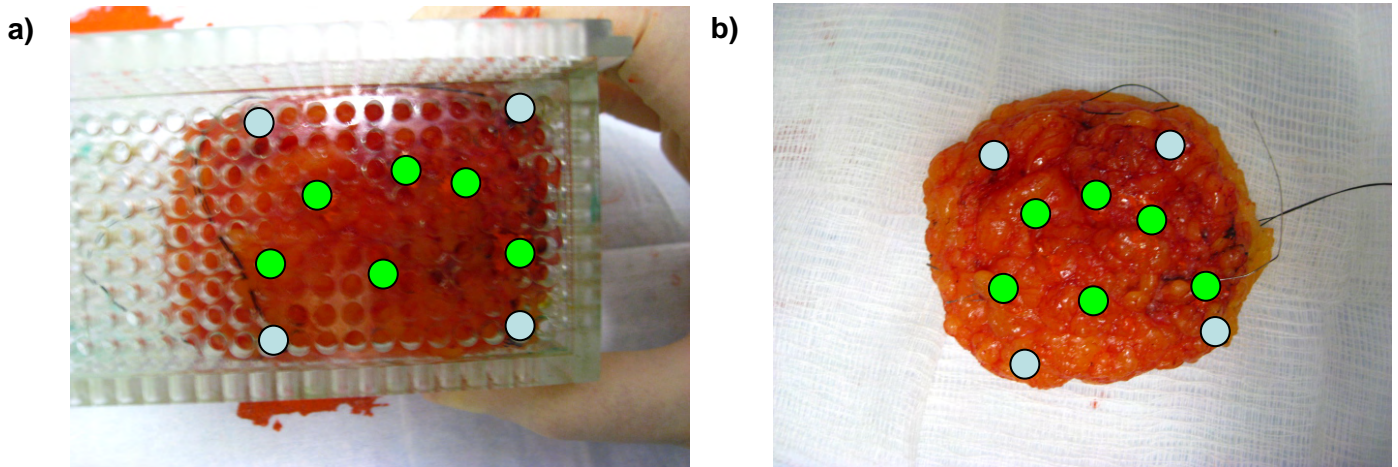


Figure 7. a) Tumor specimen inside a plexi-glass box. The 4 corners of the imaged margin are inked blue. The pathology department provides a pathological diagnosis for the area inside the blue dots; this is the margin pathology. For every specimen between 6 and 10 specific holes are inked green for pathological diagnosis on a site level basis. b) Tumor specimen after it has been imaged, inked, and removed from the plexi-glass box.

	Pathology of Measured Margin				
	Negative (Negative Specimen)	Negative (Positive Specimen)	Close	Positive	
N	15	13	14	11	53
% of margins oriented correctly for pathology	100%	77%	93%	91%	91%

Table 3. The percentage of margins oriented by our group that would be oriented the same way by trained pathology assistants.

Post-operative pathology was used as the gold standard to describe each margin as negative (malignant tissue >2mm from tissue surface), close (malignant tissue <2mm from tissue surface), or positive (malignant tissue at surface). Re-excision surgery is performed on close and positive margins so for the purposes of data analysis close and positive margins were lumped together. Table 4 is a breakdown of the imaged margins by their pathological diagnosis.

	Negative	Close	Positive	Total
Total Sample Size	30	14	11	55
Data Analysis Sample Size	15	14	11	40

Table 4. Breakdown of the number of margins imaged by their pathological diagnosis.

Diffuse reflectance spectra collected from the tissue were corrected for daily variations in optical throughput using a reflectance standard. Using an inverse Monte Carlo model, the optical properties (absorption and scattering) of the tissues were extracted from the diffuse reflectance spectra. From this we can calculate important tissue parameters such as hemoglobin saturation, total hemoglobin, oxyhemoglobin, deoxyhemoglobin, mean scattering, and beta carotene for each site on the tumor. These extracted parameters can then be used to create image maps of the tumor margin. Images have been created for each tissue parameter along with various ratios of the tissue parameters, such as the ratio of scattering to beta carotene concentration. In order to quantitatively analyze each image, simple statistics, such as calculating the mean of beta carotene, can be performed to come up with one value for each image. The simple statistics and tissue parameters found for each image are shown in Table 5. Wilcoxon Rank-Sum tests were used to determine which descriptive variables exhibit the most significant differences between path-negative and path-positive margins. Data was analyzed with two different wavelength ranges (400-600nm and 450-600nm).

Simple Statistic	Tissue Parameter
Minimum	Mean scattering
Maximum	Beta carotene
$\frac{Maximum}{Minimum}$	Oxyhemoglobin
Maximum - Minimum	Deoxyhemoglobin
Mean	Total hemoglobin
Median	Hemoglobin saturation
Variance	Total hemoglobin:Mean scattering
Coefficient of variation	Total hemoglobin:Beta carotene
$\frac{\# pixels < threshold}{total \# pixels}$	Total hemoglobin:Oxyhemoglobin
	Total hemoglobin:Deoxyhemoglobin
	Beta carotene:Mean Scattering
	Beta carotene:Oxyhemoglobin
	Beta carotene:Deoxyhemoglobin
	Beta carotene:Total hemoglobin
	Beta carotene:All absorbers
	Mean scattering:Beta carotene
	Mean scattering:Oxyhemoglobin
	Mean scattering:Deoxyhemoglobin
	Oxyhemoglobin:Deoxyhemoglobin
	Oxyhemoglobin:All absorbers
	Deoxyhemoglobin:All absorbers

Table 5. Descriptive variables used to determine differences between positive/close and negative margins.

Upon visual inspection of margin parameter images, differences can be seen between close/positive and negative margins. The images of Figure 8 a,d correspond to the ratio of scattering to beta carotene concentration in a positive and a negative margin. For the positive margin, one circled area corresponds to a path-positive site (DCIS) and the other area circled corresponds to a path-negative site (fibroadipose). The absorption and reduced scattering spectra from these two sites are seen in Figure 8 b,c. All of the pixels in the negative margin are assumed to be free of disease since pathology deemed the margin negative for residual cancer. The absorption and reduced scattering spectra from two sites with benign histopathology (one with fat and epithelial tissue and another with fat and fibroglandular tissue) are plotted in Figure 8 e,f. The positive margin has higher overall values for scattering to beta carotene than the negative margin.

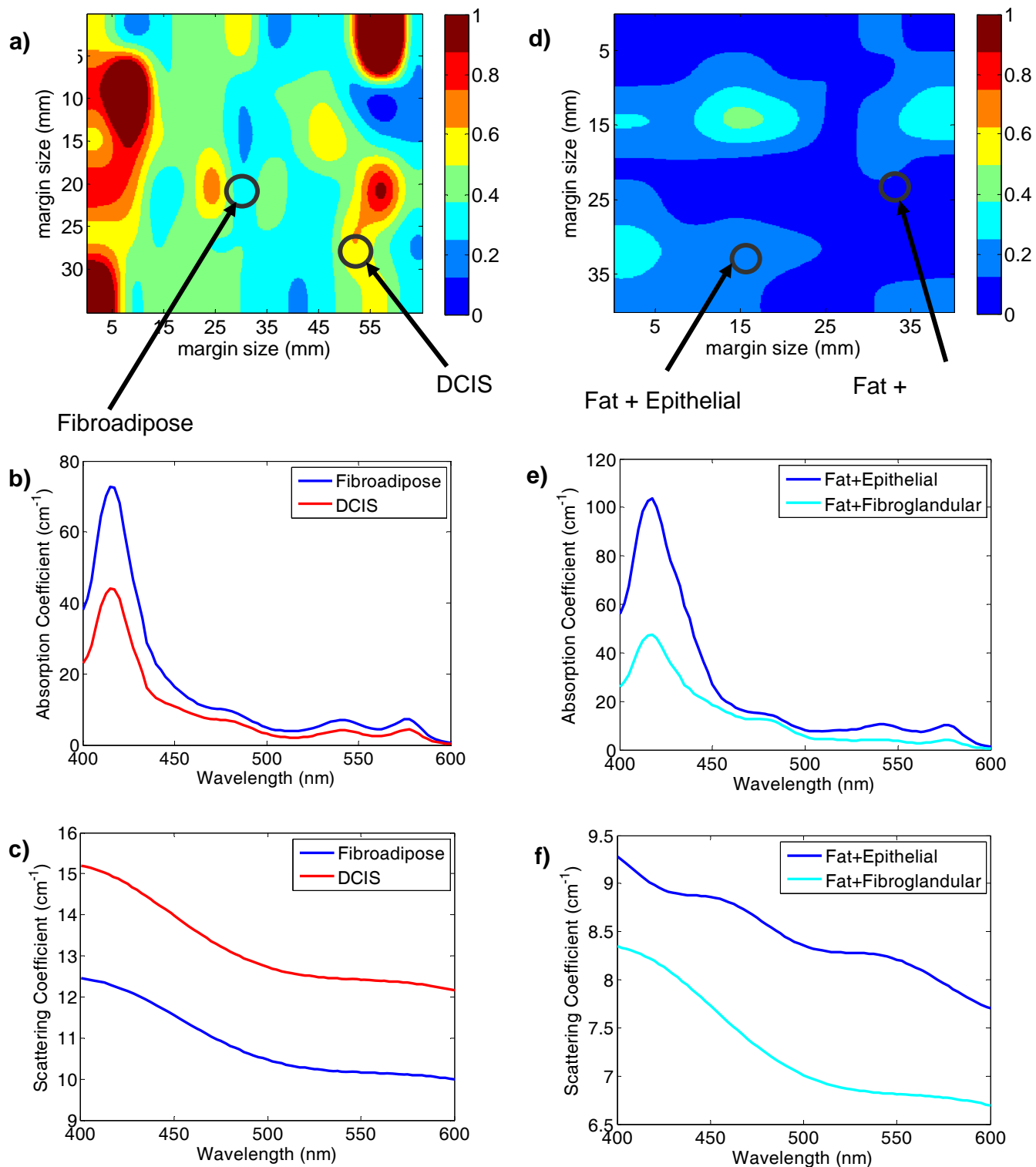


Figure 8. a) Image map of mean scattering:beta carotene for a path-positive margin with one negative site (fibroadipose) and one positive site (DCIS) circled. b) Absorption spectra of the two sites circled in a. c) Scattering spectra of the two sites circled in a. d) Image map of mean scattering:beta carotene for a path-negative margin with two different types of negative tissue

(fat+epithelial tissue and fat+fibroglandular) circled. e) Absorption spectra of the two sites circled in d. f) Scattering spectra of the two sites circled in d.

Figure 9a is an image of scattering to beta carotene from a margin with invasive ductal carcinoma (IDC) from 400-600nm. Figure 9b is the same margin but with the data from 450-600nm. Figure 9c is an image of scattering to beta carotene from a margin with ductal carcinoma in-situ (DCIS) from 400-600nm. Figure 9d is the same margin from 450-600nm. Comparing the differences between 400-600nm and 450-600nm in the images there is not much difference between the two wavelength ranges. For future experiments reducing the number of wavelengths collected during ex-vivo experiments would help to reduce the overall time required for each experiment.

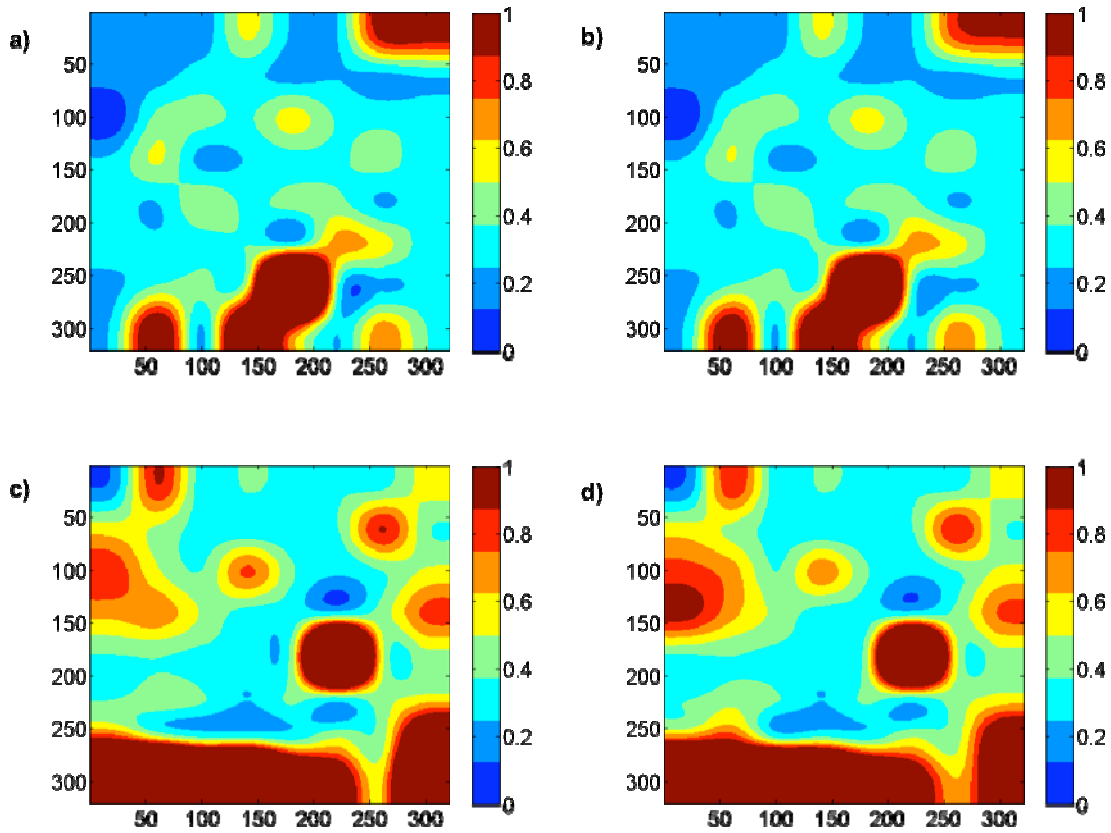


Figure 9. a) Image map of IDC from 400-600nm, b) Image map of IDC from 450-600nm, c) Image map of DCIS from 400-600nm and d) image map of DCIS from 450-600nm.

Statistically significant differences were found between close/positive (n=25) and negative (n=15) margins for many of the image descriptive variables using a Wilcoxon Rank-Sum test. The significant ($p < 0.05$) descriptive variables for analysis between 400-600nm and 450-600nm can be seen in Table 7. The direction of the arrow indicates how the mean changes from a positive margin to a negative margin (i.e. if the arrow is pointing up, the mean increases in a positive margin for that descriptive variable). From this table, we can see that for the most part the p-values are slightly lower for the 450-600nm wavelength range. The solet band of

hemoglobin is seen at ~420nm. Most of the lumpectomy specimens that are imaged can have a lot of surface blood. Eliminating the solet band from the data analysis could be helping to eliminate some of the affects of the blood, thus allowing the Monte Carlo model to more accurately fit the data.

		400 - 600 nm		450 - 600 nm	
Descriptive Variable		Direction	p	Direction	p
<i>Total Hemoglobin</i>	Pixel Percent			↑	0.0469
<i>Beta carotene</i>	Maximum	↓	0.0414	↓	0.0140
	Mean	↓	0.0337	↓	0.0293
	Median	↓	0.0473	↓	0.0387
	Pixel Percent	↑	0.0129	↑	0.0124
	Range			↓	0.0254
	Variance			↓	0.0273
<i>Total Hemoglobin Scattering</i>	Mean	↓	0.0361	↓	0.0254
	Median	↓	0.0387	↓	0.0443
	Pixel Percent	↑	0.0069	↑	0.0053
<i>Beta carotene Scattering</i>	Maximum	↓	0.0163	↓	0.0086
	Mean	↓	0.0094	↓	0.0102
	Median	↓	0.0176	↓	0.0140
	Pixel Percent	↑	0.0030	↑	0.0015
	Range	↓	0.0236	↓	0.0176
	Variance	↓	0.0163	↓	0.0140
<i>Scattering Oxyhemoglobin</i>	Median	↑	0.0443		
	Minimum			↑	0.0337
	Pixel Percent	↓	0.0487	↓	0.0371
<i>Scattering Deoxyhemoglobin</i>	Median			↑	0.0414
<i>Beta carotene Total Hemoglobin</i>	Pixel Percent	↑	0.0241		
<i>Deoxyhemoglobin All Absorbers</i>	Pixel Percent	↑	0.0185		
<i>Oxyhemoglobin All Absorbers</i>	Pixel Percent	↑	0.0209		

Table 7. Statistically significant descriptive variables calculated using a Wilcoxon Rank-Sum test between negative margins (n=15) and close/positive margins (n=25). Comparison of data analysis from 400-600nm and 450-600nm.

Figure 10 contains boxplots for three of the most significant image-descriptive variables for 400-600nm and 450-600nm. Again, there is little difference seen between the two different wavelength ranges in the boxplots.

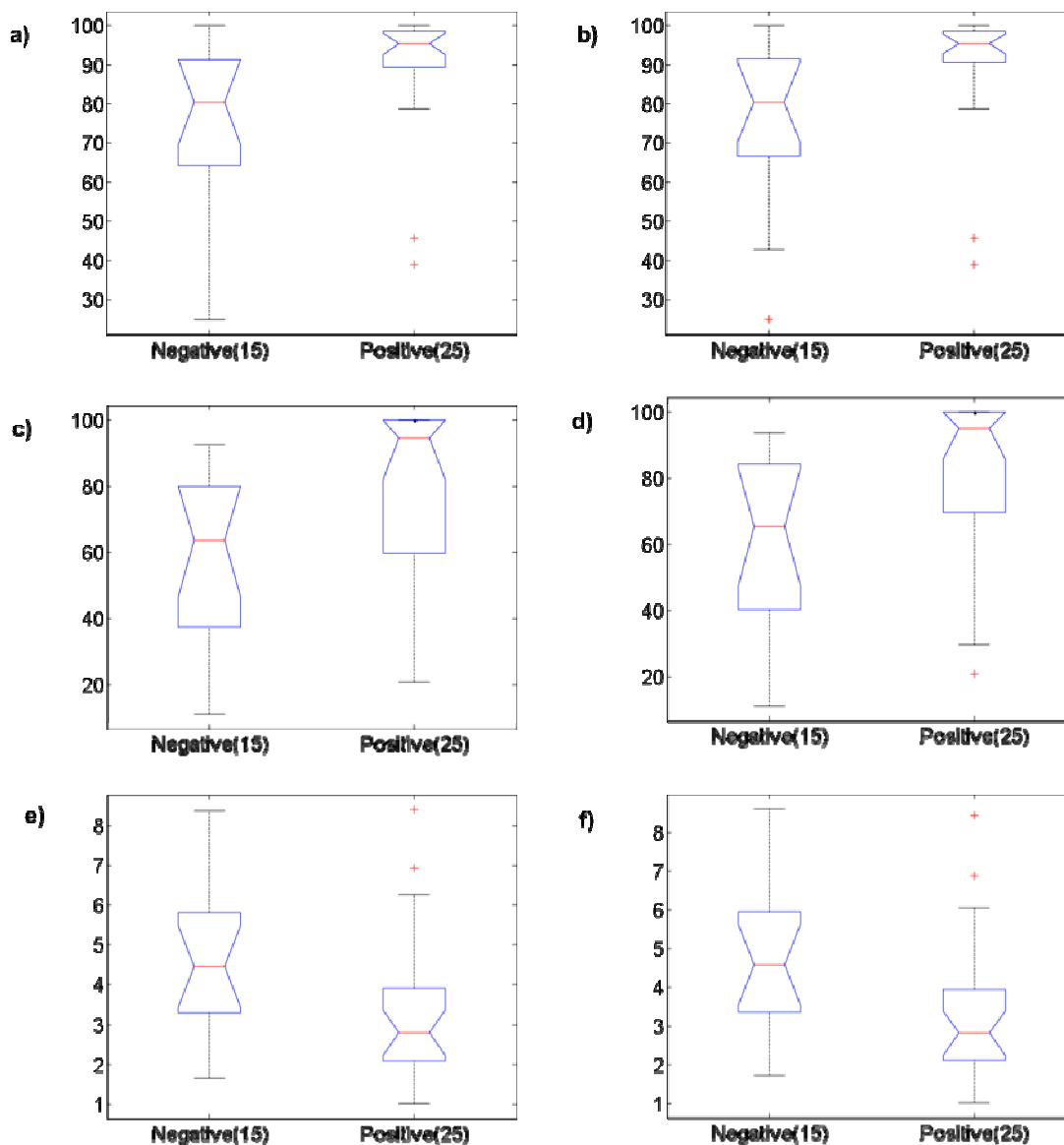


Figure 10. Boxplots of the 3 most significant variables as determined by a Wilcoxon rank-sum test. Data analyzed from 400-600nm is shown on the left, 450-600nm is shown on the right. a,b) Percentage of pixels below 16 for total hemoglobin:scattering, c,d) percentage of pixels below 5 for beta carotene:scattering, e,f) mean beta carotene:scattering.

Figure 11 shows two scatterplots of total hemoglobin to scattering versus beta carotene to scattering for 400-600nm and 450-600nm. Both scatterplots show that there is some separation between positive and negative margins and thus future margins could be predicted.

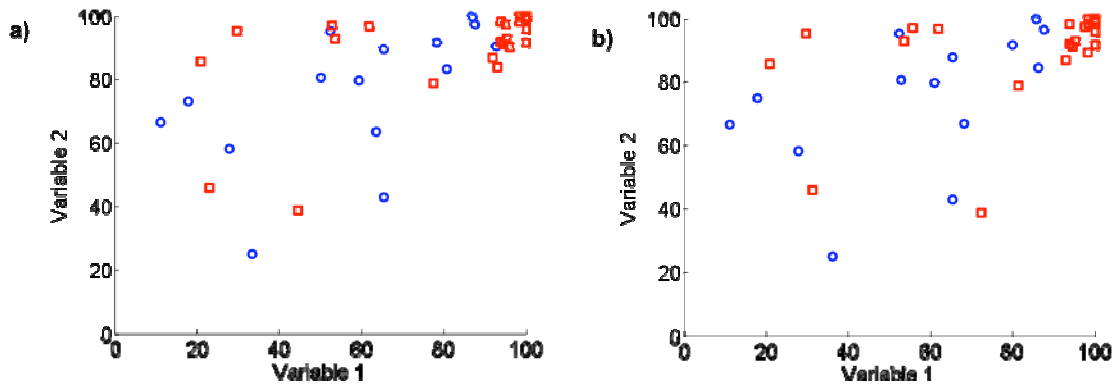


Figure 11. Scatterplot of total hemoglobin:scattering versus beta carotene:scattering. Red squares are positive margins, blue circles are negative margins.

Key Research accomplishments

- A multi-channel probe has been built
- Tissue phantom experiments have been done to show that the multi-channel probe can collect data that is repeatable and reliable
- The multi-channel probe and imaging system have been used to collect data from 43 patients
- Statistically significant differences can be seen between negative and positive surgical margins

Reportable Outcomes

Conclusions

The outcome of the proposed work is expected to result in a new optical diagnostic modality for breast cancer margin assessment at the time of tissue removal. A clinical procedure has been put in place and data has been collected from several patients at this point. Statistically significant differences can be seen between negative and positive margins. Data from 7 more patients still needs to be collected to complete Task 4. The goal of Task 5 is to create a predictive model that will allow surgical margins to be diagnosed during surgery. The final spectroscopic imaging device will result in cosmetically-superior lumpectomies at the time of the first surgery, better margin assessment leading to reduced repeat surgeries and hence, reduced local recurrence, emotional distress, and complications due to reduced number of surgeries and shorter recovery times for the patient.

References

1. American Cancer Society, 2008.
2. American Cancer Society. Cancer Facts and Figures. 2005.
3. Morrow M WJ, Moughan J, et al. . Factors Predicting the Use of Breast-conserving therapy in Stage I and II breast carcinoma. Journal of Clinical Oncology 2001; 19:2254-2262.
4. Jacobs, Lisa. Positive Margins: The Challenge Continues for Breast Surgeons, Annals of Surgical Oncology, 15:1271-1272, May 2008.
5. Palmer GM, and N. Ramanujam. A Monte Carlo based inverse model for calculating tissue optical properties, part I: Theory and validation on synthetic phantoms. Applied Optics 2006; 45(5):1062-1071.
6. Palmer GM, C. Zhu, T.M. Breslin, F. Xu, K.W. Gilchrist, and N. Ramanujam. A Monte Carlo based inverse model for calculating tissue optical properties, part II: Application to breast cancer diagnosis. Applied Optics 2006; 45(5):1072-1078.
7. Zhu C, Palmer GM, Breslin TM, Harter J, Ramanujam N. Diagnosis of breast cancer using diffuse reflectance spectroscopy: Comparison of a Monte Carlo versus partial least squares analysis based feature extraction technique. Lasers Surg Med 2006; 38(7):714-724.

Appendix

1. Revised Statement of Work

Statement of Work

Near Infrared Spectroscopy for Improving Breast Core Needle Biopsy
Torre Michelle Bydlon, Investigator – Predoctoral Award Applicant

Task 1: Conceptual design of a spectroscopic imaging device (system and fiber optic probe)
(Months 1 – 10)

- a. Design an imaging system (Months 1 – 10)
- b. Determine the appropriate number of channels for the imaging probe (Months 8 – 10)
 - i. Dependent on cross-talk at the tissue surface, number of collection fibers that can be imaged on the CCD (charge coupled device), and number of illumination fibers that can be illuminated by the light source
- c. Determine the number of collection fibers that can be imaged on a variety of CCDs with different pixel sizes and calculate the throughput of the entire imaging system with the various CCDs (Months 8 – 10)
 - i. Select a CCD to purchase for the imaging system
- d. SNR (signal to noise ratio) calculations to determine the appropriate spacing between each channel (Months 8 - 10)

Successful completion of this task will result in a design of an imaging system. The design for an imaging probe will also be complete and ready to build ourselves or by an industry partner.

Task 2: Build and test a two channel imaging probe (Months 11 – 14)

- a. Build an imaging probe with two channels where the channels have no specified separation distance (Months 11-12)
- b. Check that there is no crosstalk between signals on the CCD (Month 12)
- c. Using a liquid phantom, fix one channel in the center of the phantom and alter the separation distance between the fixed channel and the second channel to test the crosstalk between the two channels and compare to simulated results from Task 1 (Months 13 – 14)
- d. Repeatability of the probe (Months 13 – 14)
 - i. A single channel will be placed in a phantom and 10 serial measurements will be made
 - ii. Mean and standard deviation will be calculated for the 10 measurements at each wavelength
 - iii. SNR will be calculated as the mean divided by the standard deviation
- e. Run an inverse Monte Carlo model, developed by our group, to determine how well the probe can extract known optical properties from tissue phantoms of hemoglobin and polystyrene spheres (Months 13 – 14)

Completing this task will allow us to determine how far apart each channel must be to avoid crosstalk on the tissue side of the probe. This will also allow us to determine how efficiently the two channel probe is. If there is insufficient signal we may have to redesign

the probe with greater separation distances between the illumination and collection fibers. We will also be able to tell if a self calibrating fiber is better than our current techniques of using an integrating sphere, puck, and water measurements to calibrate data. Completing the Monte Carlo inversions with two channels will help us to determine what difficulties we will face when trying to run the inversions with multiple channels and try to make the code more efficient at analyzing large amounts of data.

Task 3: Build a 25 channel imaging probe and system (Months 15 – 17)

- a. Build imaging probe
 - i. Provide one of our industry partners, Romack or Polymicro, with our design specifications or build the probe ourselves
 - ii. The probe specifications will be based on results that we find from the 2-channel probe tests
- b. The imaging system will consist of a monochromator, lens system for focusing and magnification of the signals from the probe, and a CCD.

Completion of this task will result in an optical spectral imaging system that will map out optical properties of turbid media and a probe to be used in tissue phantom studies and/or a clinical setting.

Task 4: Test imaging probe and system (Months 18 – 38)

- a. Complete a number of tissue phantom studies to characterize the system (Months 18 – 21)
- b. Analyze the phantom data by running an inverse Monte Carlo model to extract the optical properties of the phantoms and compute errors between the extracted values and the actual optical properties (Months 18 – 22)
- c. Complete an ex-vivo tissue analysis in the clinic with human subjects undergoing breast reduction surgery (Months 23 – 38)
 - i. Collect optical spectral images from 50 partial mastectomy specimens
 - ii. Extract the absorption and scattering coefficients from the optical spectra using an inverse Monte Carlo model
 - iii. Compare extracted tissue properties to histopathology obtained for each margin imaged

Successful completion of this task will determine how accurate the imaging probe and system are at extracting optical properties of phantom tissue data as well as human tissue data.

Task 5: Create a predictive model to diagnose surgical margin status (Months 24 – 38)

- a. Create image maps of the extracted parameters and determine which parameters are statistically significant

- b. Create a multivariate predictive model based on the statistically significant parameters; test the accuracy of this model by using a leave-one-out cross validation technique
- c. Prospective clinical study
 - a. Test the predictive model on 30 positive margins
 - b. Determine the re-excision rate with the use of the imaging device as a tool in the operating room

Successful completion of this task will result in a model that can be used to diagnose surgical margin status in the operating room.

*** Month 1 began September 2006